Astron. Astrophys. 334, 439–452 (1998)

ASTRONOMY
AND
ASTROPHYSICS

Probing nuclear starburst activity in a sample of nearby spiral galaxies⋆

C. Bonatto[1], **M.G. Pastoriza**[1], **D. Alloin**[2], **and E. Bica**[1]

[1] Universidade Federal do Rio Grande do Sul, IF, CP 15051, Porto Alegre 91501–970, RS, Brazil
[2] CNRS URA 2052, SAp CE-Saclay, Orme des Merisiers Bât 709, F-91191 Gif-Sur-Yvette Cedex, France

Received 31 October 1997 / Accepted 9 March 1998

Abstract. As part of a systematic study of the UV properties of galaxies in the IUE library, we present in this paper an analysis of nuclear stellar populations in spiral galaxies with radial velocity $\leq 5\,000\,\mathrm{km\,s^{-1}}$. In this sample of 60 galaxies the IUE aperture probes a mean 1.0 kpc × 2.1 kpc area. Prior to any comparison of galaxy spectra in the range covered by IUE (1200–3200 Å), we have formed subsets according to the absolute magnitude and morphological type of the studied galaxies. In a second step, and within each subset, we have co-added the spectra, and hence the objects into groups of similar spectral properties in the UV, also taking into account their spectral properties in the visible/near-infrared ranges. As a result, high signal-to-noise ratio templates have been obtained, and information on spectral features can now be extracted and interpreted. We distinguish 4 groups for Sa, 8 for Sb, and 4 for Sc galaxies. We have carried out population syntheses using as base elements: H II regions, integrated star clusters, and far-UV weak elliptical galaxies as representative of bulge stellar population. The variety of UV spectral types found in the central regions of spiral galaxies can be readily explained by different mixtures of bulge, circumnuclear burst and disc populations. Across different morphological types, similar templates can also be found. This is due to compensation effects of bulge contribution with the disc and circumnuclear burst ones. Flux fractions derived from the population synthesis have been converted into mass contributions and inferences have been made on the star-formation histories. In the central kpc of the galaxies with strong UV flux, we find that the mass stored in the young components ($t < 500$ Myr) is typically $\approx 10^7\,M_\odot$. We confirm that such star-formation enhancements occur preferentially in barred spirals. Internal reddening in the templates has been studied and inferences have been made on the corresponding reddening laws. We find cases where an SMC-like law applies and others where a faint $\lambda 2200$ Å absorption feature occurs resembling the reddening law of the LMC. The interest of the IUE data set resides in its rather large entrance aperture which samples a large portion of nearby galaxies, and is therefore quite suitable for the interpretation of large redshift galaxies.

Key words: galaxies: spiral – galaxies: starburst – galaxies: stellar content – galaxies: nuclei – ultraviolet: galaxies

1. Introduction

In view of extending to the UV the wavelength range over which one is able to perform population synthesis of galaxies, we started a programme using the IUE database. The problem of signal-to-noise (S/N) limitations in IUE data was minimized by grouping objects with similar UV properties. This procedure has been applied already in the case of integrated star cluster spectra (Bonatto, Bica & Alloin 1995) and is described in detail in this paper (hereafter referred to as Paper I).

Regarding galaxies, several studies of IUE spectra by object class have already been carried out, e.g. the spectral atlases of Kinney et al. (1993) for star-forming galaxies, and of Rosa, Joubert & Benvenutti (1984) for H II complexes. Besides, we have applied our grouping procedure to derive UV properties of early-type galaxies, elliptical and S0s, in Bonatto et al. (1996, hereafter referred to as Paper II). The interpretation of the UV-turnup in some ellipticals has been extensively discussed by Bica et al. (1996).

Stellar populations in the central regions of spiral galaxies have not yet been fully explored in the UV. Some efforts were dedicated to specific galaxies, e.g. Ellis, Gondhalekar & Efstathiou (1982) who studied the nuclei of NGC 4594,3031,5194 and 4258 in conjunction with data at other spectral wavelengths. Detailed studies have been performed on the nucleus of M 31 (e.g. Welch 1982). Recently, Ferguson & Davidsen (1993) studied the central region of M 31 down to the Lyman limit using the Hopkins Ultraviolet Telescope (HUT). Nowadays, the high spatial resolution of the Hubble Space Telescope (HST) allows a more direct approach to the problem and has allowed to discover super-star clusters in circumnuclear bursts (hereafter referred to as CNBs) of several galaxies: NGC 1097 and NGC 6951 (Barth et al. 1995), NGC 3310 and NGC 7552 (Meurer et al. 1995), and NGC 1079,1433,1512 and NGC 5248 (Maoz et al. 1996).

In the present work we apply the grouping method to the sample of spiral galaxies available in the IUE database. Spectra showing important signs of activity (type 1 and 2 Seyferts) have been discarded. The resulting spectral groups are interpreted in

Send offprint requests to: M.G. Pastoriza

⋆ Based upon data collected with the International Ultraviolet Explorer (IUE) Satellite, supported by NASA, SERC and ESA.

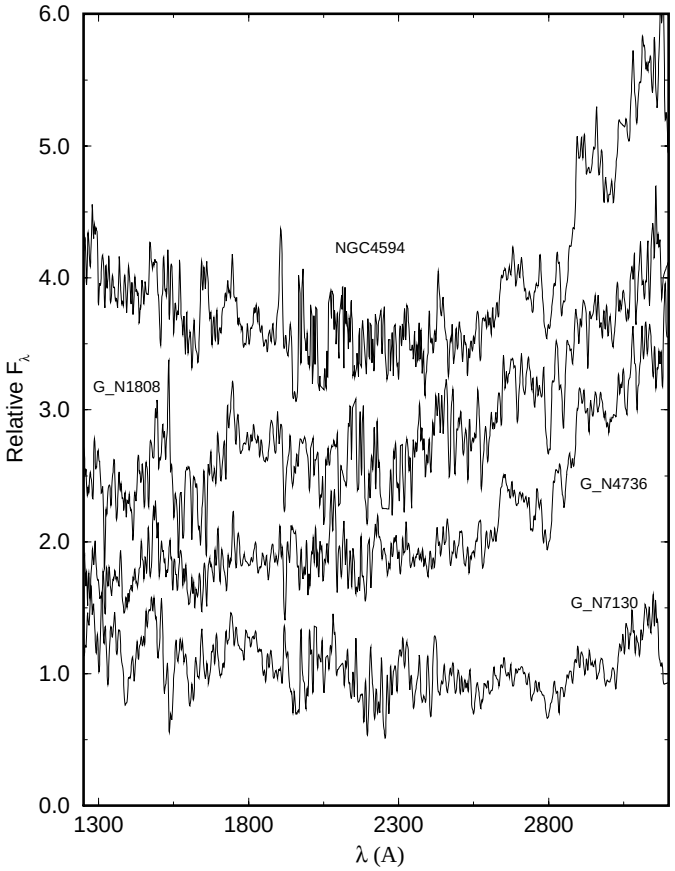

Fig. 1. Spectral groups for Sa galaxies. Flux in F_λ units, normalised to 1.0 at $\lambda 2646$ Å. Except for the bottom one, the spectra have been shifted by an arbitrary amount, for clarity purposes.

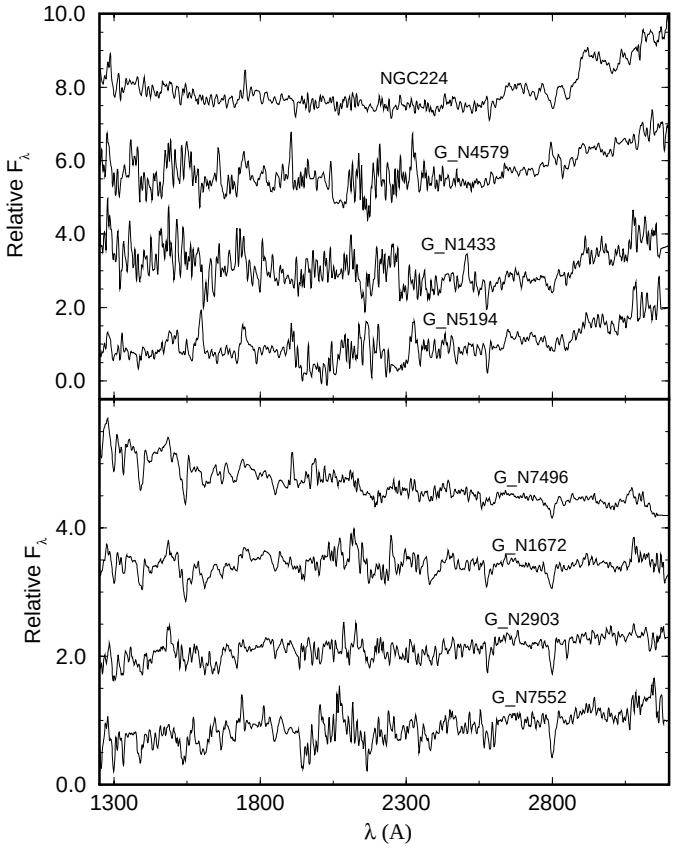

Fig. 2. Same as Fig. 1 for the spectral groups of Sb galaxies. Galaxy groups with a percentage of bar occurrence larger than 80% in the galaxies forming the group, are gathered in the lower panel.

terms of age components, as well as reddening effects, making use of a base of star cluster and galaxy templates with known properties.

Among others, one goal of this work is to test the possible rôle played by bars in generating CNBs in the central regions of spiral galaxies. The effect of bars was already pointed out by Pastoriza (1975 and references therein) on the basis of visible spectra and images. It has also been predicted by theoretical analyses and numerical simulations of the dynamics in the central regions of spiral galaxies (Athanassoula 1992, Martin 1995, Piner, Stone & Teuben 1995, Elmegreen 1996).

In Sect. 2 we introduce the present sample of nuclear stellar populations in spiral galaxies. We group the objects according to spectral similarities in Sect. 3, where we also present equivalent width and continuum measurements for the different galaxy groups. We carry out population syntheses for the groups and discuss the results in Sect. 4. The rôle of bars in powering nuclear bursts is discussed in Sect. 5. Finally, the conclusions of this work are given in Sect. 6.

2. Data set

The spectra have been extracted from the IUE database stored at the Instituto Astronômico e Geofísico of the Universidade de São Paulo. We have selected the available SWP, LWP and LWR spectra of spiral galaxies obtained with the large aperture ($10'' \times 20''$). The objects used in this analysis, along with other relevant data are presented in Tables 1, 2 and 3, respectively for Sa, Sb and Sc galaxies. Only objects with a morphological type T$\geq$0 have been retained (de Vaucouleurs et al. 1991, hereafter RC3). We have gathered in Tables 1, 2 and 3 the following information, by columns: (1) alternative identifications; (2) PGC number; (3) morphological type (T), and presence of a bar indicated by B; (4) foreground absorption A_B; (5) total blue magnitude B_T; (6) M_B assuming $H_O = 75\,\mathrm{km\,s^{-1}\,Mpc^{-1}}$; (7) heliocentric radial velocity, and (8) complementary remarks. Absolute magnitudes M_B were calculated using Galactic standard of rest (V_G) velocities (RC3), while optical and H I heliocentric velocities (V_R) were considered for redshift corrections of the IUE spectra. The main sources (and references therein) were: RC3 (identifications, PGC number, T, V_R, A_B, B, V_G for M_B calculations); Sandage & Tammann (1981) for V_G in some groups of galaxies; Mazzarella & Balzano (1986) for data on Markarian galaxies. We also searched the NASA/IPAC Extragalactic Database (NED)[1] for complementary information. Ad-

[1] The NASA/IPAC Extragalactic Database (NED) is operated by the Jet Propulsion Laboratory, California Institute of Technology, under contract with the National Aeronautics and Space Administration.

Table 1. Sa galaxies

Group/Object	PGC #	T	A_B mag	B_T mag	M_B mag	V_R $\mathrm{km\,s^{-1}}$	Remarks
NGC 4594 — important bulge stellar population and moderate UV flux							
M 104, NGC 4594, MCG-02-32- 20, IRAS 12373-1120	42407	1.0	0.13	8.98	-22.5	1082	bulge pop
G_N1808 — reddened nuclear starburst							
NGC 1808, ESO 305-G8, IRAS 05059-3734	16779	1.0 B	0.07	10.45	-19.6	749	CNB
NGC 2681, UGC 4645, ARK 185	24961	0.0 B	0.10	10.88	-19.0	683	
G_N7130 — moderate bulge stellar population and moderate UV flux							
NGC 2639, UGC 4544, IRAS 08400+5023	24506	1.0	0.11	12.19	-21.1	3198	
NGC 2798, UGC 4905, IRAS 09141+4212, in ARP 283	26232	1.0 B	0.00	12.48	-19.3	1734	in pair, disturbed
NGC 3682, UGC 6459, IRAS 11247+6651	35266	0.0	0.00	13.12	-18.3	1543	
NGC 4314, UGC 7443, IRAS 12200+3010	40097	1.0 B	0.09	11.17	-19.5	963	
NGC 4500, Mrk 213, UGC 7667	41436	1.0 B	0.00	13.03	-20.1	3115	BCG
NGC 7130, IC 5135, ESO 403-G32, IRAS 21453-3511	67387	1.0	0.00	12.88	-21.1	4791	pec, in cluster
NGC 7172, ESO 466-G38, IRAS 21591-3206	67874	1.4	0.00	12.54	-20.1	2569	in cluster
NGC 7233, ESO 289-IG8, IRAS 22127-4605	68441	0.0 B	0.00	12.90	-19.0	1795	in pair
G_N4736 — important bulge stellar population and weak UV flux							
M 64, NGC 4826, UGC 8062, IRAS 12542+2157	44182	2.0	0.16	8.82	-20.4	480	
M 94, NGC 4736, UGC 7996, IRAS 12485+4123	43495	2.0	0.00	8.75	-19.2	297	

Table Notes. B in column 3 identifies the galaxies with bars; CNB identifies the presence of circumnuclear burst.

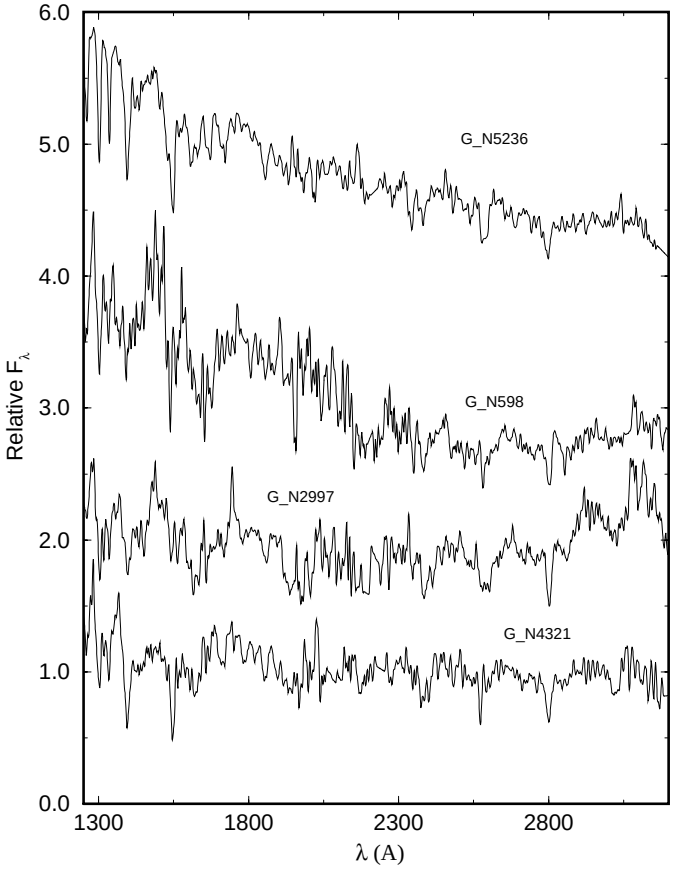

Fig. 3. Same as Fig. 1 for the spectral groups of Sc galaxies.

ditional relevant references are given in Sect. 3. The A_B values were used to correct all spectra for the foreground (Galactic) reddening using Seaton's law (1979) and $A_B/E(B-V) = 4.0$. Thus, in the subsequent analyses all spectra are corrected for *foreground reddening and redshift.*

3. Galaxy spectral groups

The spiral galaxies in this sample exhibit a wide range of spectral properties. We first grouped galaxies according to morphological type and luminosity, in order to ensure that a bulge contribution of similar nature (in terms of metallicity, for example) is enclosed within the IUE aperture ($10'' \times 20''$); notice that the galaxy sample is restricted to radial velocities $V_R < 5\,000\,\mathrm{km\,s^{-1}}$. This bulge contribution — with respect to the total flux — may however vary slightly within each group, as a result of the spread in distance among the objects forming each group. The subsequent grouping parameter was a "direct" one: similarity of the IUE spectra in terms of the spectral energy distribution and absorption features. This procedure allows one to study average properties of the resulting group spectra with an improved signal to noise (S/N) ratio. Details on the co-adding method are fully described in Papers I and II. In Tables 1, 2 and 3 the galaxies are organized according to this grouping.

The resulting groups with the galaxies they are built of, along with the number of SWP and LWP/LWR spectra effectively used for each galaxy, are presented in Tables 4, 5 and 6 respectively for Sa, Sb and Sc galaxies. Each spectral group is named after a member which has spectra both in the SWP and LWP/LWR domains with a good (S/N) ratio. The projected IUE aperture in kpc is shown in Tables 4, 5 and 6 for individual galaxies as well as the respective mean values for the groups. Averaging the projected aperture over the present sample (60 galaxies) results in 1.0 kpc $\times$ 2.1 kpc. Thus what we study here is the integrated spectrum of the highest surface brightness regions of nearby spiral galaxies, which is essential for comparison with the spectra of distant galaxies. We also recall in Tables 4, 5 and

Table 2. Sb galaxies

Group/Object	PGC #	T	A_B mag	B_T mag	M_B mag	V_R $\mathrm{km\,s^{-1}}$	Remarks
NGC 224 — important bulge stellar population and moderate UV flux							
M 31, NGC 224, UGC 454	2557	3.0	0.33	3.36	-21.1	-226	
G_N4579 — same as NGC 224 with additional weak emission lines							
M 58, NGC 4579, UGC 7796, VCC 1727	42168	3.0 B	0.15	10.29	-20.5	1917	
M 88, NGC 4501, UGC 7675, VCC 1401	41517	3.0	0.10	9.86	-20.9	1016	
G_N7552 — reddened nuclear starburst							
M 90, NGC 4569, UGC 7786, in ARP 76	42089	2.0 B	0.09	9.79	-21.0	-222	in pair
NGC 7552, ESO 291-G12, IRAS 23134-4251, IC 5294	70884	2.0 B	0.04	11.13	-20.6	1653	CNB, in group
NGC 7582, ESO 291-G16, IRAS 23156-4238	71001	2.0 B	0.04	10.83	-20.8	1564	in group
G_N1433 — moderate bulge stellar population and moderate UV flux							
NGC 1433, ESO 249-G14, IRAS 03404-4722	13586	2.0 B	0.00	10.64	-19.9	972	CNB
NGC 2841, UGC 4966, IRAS 09185+5111	26512	3.0	0.00	9.58	-20.0	635	
NGC 4102, UGC 7096, IRAS 12038+5259	38392	3.0 B	0.01	11.61	-18.7	877	
G_N1672 — nuclear starburst: flat spectrum							
M 95, NGC 3351, UGC 5850, IRAS 10413+1158	32007	3.0 B	0.05	10.26	-19.9	771	CNB
NGC 245, Mrk 555, UM274, UGC 476	2691	3.0	0.07	12.79	-21.0	4082	
NGC 1097, ESO 416-G20, ARP 77	10488	3.0 B	0.03	9.92	-21.2	1274	CNB, in pair
NGC 1672, ESO 118-G43, IRAS 04449-5920	15941	3.0 B	0.00	10.25	-20.9	1282	CNB
NGC 2146, UGC 3429, IRAS 06106+7822	18797	2.0 B	0.33	10.58	-20.1	873	pec
NGC 6300, ESO 101-G25, IRAS 17123-6245	60001	3.0 B	0.52	10.20	-21.0	1048	
NGC 6500, UGC 11048, IRAS 17537+1820	61123	1.7	0.40	12.46	-20.9	2955	
NGC 6764, UGC 11407, IRAS 19070+5051	62806	3.5 B	0.25	12.14	-20.6	2390	
G_N7496 — very blue nuclear starburst							
NGC 3049, Mrk 710, UGC 5325	28590	2.0 B	0.04	12.77	-18.7	1439	
NGC 3504, UGC 6118, IRAS 11004+2814	33371	2.0 B	0.02	11.56	-20.0	1518	CNB
NGC 3982, UGC 6918, IRAS 11538+5524	37520	3.0 B	0.00	11.68	-18.8	924	
NGC 5430, Mrk 799, UGC 8937	49881	3.0 B	0.00	12.31	-20.7	3028	in pair
NGC 7496, ESO 291-G01, IRAS 23069-4341	70588	3.0 B	0.00	11.84	-19.7	1527	in group
NGC 7714, Mrk 538, UM 167, UGC 12699, in ARP 284	71868	3.0 B	0.16	12.62	-20.4	2808	Sdm pec, in pair
G_N5194 — important bulge stellar population and moderate UV flux							
M 51, NGC 5194, UGC 8493, in ARP 85	47404	4.0	0.00	8.67	-20.2	450	in pair
M 63, NGC 5055, UGC 8334	46153	4.0	0.00	9.03	-20.1	510	
NGC 5005, UGC 8256, IRAS 13086+3719	45749	4.0 B	0.00	10.19	-20.5	1022	
G_N2903 — reddened nuclear starburst							
NGC 253, ESO 474-G29	2789	5.0 B	0.05	7.09	-20.9	140	
NGC 2903, UGC 5079	27077	4.0 B	0.07	9.11	-20.4	565	CNB

Table Notes. B in column 3 identifies the galaxies with bars; CNB identifies the presence of circumnuclear burst.

6 the galaxy membership in templates of nuclear stellar populations in spiral galaxies, from the visible and near-IR ranges, for which Bica (1988) carried out population syntheses: S 1 and S 3 are red stellar populations typical of bulges, S 1 being the most metal-rich. Templates S 5 and S 7 contain recent star-formation components, more important in S 7. We show the spectra of the resulting groups in Figs. 1, 2 and 3, respectively for Sa, Sb and Sc galaxies.

3.1. Measurements

In Paper I we defined a series of windows and regions in the UV which are suitable for measuring equivalent widths (EW) and continuum points. In Table 7 we present EWs for the UV windows measured in the various spectral groups. The number and wavelength limits of the UV windows (as defined in Paper I), together with the main absorbers in each window, are recalled in the first three columns of Table 7, respectively. Continuum points, normalised at $\lambda 2646$ Å, are also provided in Table 7.

4. Population syntheses in the UV

As emphasised already (e.g. Bica 1988, Alloin & Bica 1990), population synthesis is better constrained by considering a wavelength range as wide as possible. Therefore, the ideal procedure would be to link, for each galaxy group template and each star cluster template, the UV spectrum discussed in this paper to that obtained over the visible domain (e.g. 3700–9500 Å, Bica 1988; 3000–4000 Å, Bica et al. 1994). One difficulty, however, in establishing this link is that the IUE entrance aperture is $10'' \times 20''$, while the one used for the visible and near-infrared domains was approximately $4'' \times 8''$ (Bica & Alloin 1987a,

Table 3. Sc galaxies

Group/Object	PGC #	T	A_B mag	B_T mag	M_B mag	V_R $\mathrm{km\,s^{-1}}$	Remarks
G_N2997 — moderate bulge stellar population and moderate UV flux							
M 101, NGC 5457, UGC 8981, ARP 26	50063	6.0 B	0.00	8.21	-20.2	221	
M 106, NGC 4258, UGC 7353, VV 448	39600	4.0 B	0.00	8.53	-20.5	480	CNB
Mrk 12, MCG+12-8-0013, UGC 4028	21971	5.0 B	0.10	12.83	-20.9	3993	in pair
NGC 1667, MCG-01-13- 13, IRAS 04461-0624	16062	5.0 B	0.24	12.41	-21.7	4555	
NGC 2403, UGC 3918, IRAS 07321+6543	21396	6.0 B	0.17	8.43	-19.3	-141	
NGC 2997, ESO 434-G35	27978	5.0	0.54	9.34	-22.0	1090	CNB
NGC 6221, ESO 138-G3, IRAS 16484-5908	59175	5.0 B	0.86	9.77	-22.4	1350	in group
NGC 7590, ESO 347-G33, IRAS 23161-4230	71031	4.0	0.04	11.46	-20.0	1465	in pair
G_N4321 — nuclear starburst: flat spectrum							
M 100, NGC 4321, UGC 7450, VCC 596	40153	4.0 B	0.06	9.98	-20.8	1219	CNB
NGC 931, Mrk 1040, UGC 1935	9399	4.0	0.32	12.23	-22.2	4914	in pair
NGC 3994, UGC 6936, ARK 337, in ARP 313	37616	5.0	0.02	13.18	-19.9	3096	S?, in pair
NGC 4244, UGC 7322, IRAS 12150+3804	39422	6.0	0.00	9.28	-18.2	240	
NGC 6217, UGC 10470, ARP 185	15538	4.0 B	0.15	11.66	-19.8	1377	
G_N598 — blue stellar population							
M 33, NGC 598, UGC 1117	5818	6.0	0.19	5.75	-19.0	-204	
NGC 7793, ESO 349-G12, IRAS 23552-3252	73049	7.0	0.02	9.37	-18.5	216	
G_N5236 — very blue nuclear starburst							
M 83, NGC 5236, ESO 444-G81, IRAS 13342-2933	48082	5.0 B	0.15	7.98	-19.8	503	in group, CNB
NGC 3310, UGC 5786, ARP 217	31650	4.0 B	0.00	10.95	-19.7	1018	CNB
NGC 3395, UGC 5931, ARK 257, in ARP 270	32424	6.0 B	0.00	12.09	-19.6	1616	in pair, disturbed
NGC 7673, Mrk 325, UGC 12607, IVZw 149	71493	5.0	0.16	12.86	-20.6	3379	in pair

Table Notes. B in column 3 identifies the galaxies with bars; CNB identifies the presence of circumnuclear burst.

1987b). For this reason, the simplest approach is to perform an independent population synthesis in the UV range, using the same method for all the groups.

Following Bica (1988, see also Schmitt, Bica & Pastoriza 1996), we have adapted the population synthesis algorithm to the UV range. Basically the algorithm uses EWs of the most prominent absorption features and selected continuum points observed in a given spectrum, and compares them to those of a model computed from a base of simple stellar population elements. The algorithm is not a minimization procedure, instead it generates all combinations of the base elements according to a given flux contribution step and compares the resulting EWs and continuum points to the input ones. The code successively dereddens galaxy input continuum points and tests them against a given base model. The possible solutions within error bars are averaged out, and this average is adopted as the final synthesis solution.

A typical synthesis includes 7 age components (Table 8). Initially, we used a 10% step for testing flux contributions at $\lambda 2646$ Å, generating about 8000 combinations for each assumed $E(B-V)$. Typically, for the appropriate $E(B-V)$, only 5% of these 8000 combinations are solutions within the error windows. Reddenings were tested in the range $0.0 < E(B-V) < 1.0$ with a step of 0.05. Thus, in total, $\approx 160\,000$ combinations are tested for each group, and the number of possible solutions amounts to less than 1%. Usually, solutions are also found for $\Delta E(B-V) = \pm 0.05$, around the best value of $E(B-V)$. Finally, after probing as above the space of combinations, we calculate the final solution with finer steps of 5% for flux contributions and $\Delta E(B-V) = 0.02$. The results are given in Table 9.

The base elements that we use in the present UV synthesis are taken from the star cluster population templates described in Paper I to represent young and intermediate age components, and from a galaxy template assumed to represent an old metal-rich bulge (Paper II). EWs and continuum points of the H II region template are measured on an average spectrum of the M 101, M 33, LMC and SMC H II region groups from Paper I. For young and intermediate age cluster elements, we use LMC groups with ages $\approx 10, 25, 75, 200$ and 1200 Myr (respectively the groups I, II, III, IVA and V in Paper I). Finally, we use a bulge template (named E2E5 by Bica and collaborators — see the database in Leitherer et al. 1996), which is the average of the far-UV weak elliptical galaxy groups G_N1553 and G_N3115 (Paper II). EWs and continuum points for these base elements are listed in Table 8.

We tested the Galactic (Seaton 1979), LMC (Fitzpatrick 1986) and SMC (Prévot et al. 1984) reddening laws for each synthesis, according to the strength of the $\lambda 2200$ Å feature.

The results of our synthesis are given in Table 9 for the Sa, Sb and Sc groups, where we present the percentage contribution of each base element to the flux at $\lambda 2646$ Å. The values of $E(B-V)$ are also given in the table. They correspond to the LMC law, except for a few cases where the SMC law turned out to be more suitable. It is interesting to point out that in no case Seaton's Galactic reddening law describes these external

Table 4. Sa galaxy groups

Galaxy	SWP	LWP/R	slit (kpc × kpc)	Spectral Type
Important bulge stellar population and moderate UV flux				
	NGC 4594		$\langle 0.7 \times 1.4 \rangle$	
M 104	3	4	0.7×1.4	T–S 1
Reddened nuclear starburst				
	G_N1808		$\langle 0.5 \times 1.0 \rangle$	
NGC 1808	1	1	0.5×1.0	
NGC 2681	1	2	0.4×0.9	
Moderate bulge stellar population and moderate UV flux				
	G_N7130		$\langle 1.6 \times 3.2 \rangle$	
NGC 2639	1	1	2.1×4.1	
NGC 2798	2	1	1.1×2.2	
NGC 3682	1	1	1.0×2.0	
NGC 4314	1	2	0.6×1.2	
NGC 4500	2	1	2.0×4.0	
NGC 7130	1	1	3.1×6.2	
NGC 7172	—	1	1.7×3.3	
NGC 7233	1	1	1.2×2.3	
Important bulge stellar population and weak UV flux				
	G_N4736		$\langle 0.3 \times 0.5 \rangle$	
M 64	2	1	0.3×0.6	
M 94	6	4	0.2×0.4	

Table Notes. Columns 2 and 3 give the number of IUE spectra effectively used; column 4 gives the projected IUE aperture ($10'' \times 20''$) in kpc × kpc; column 5 recalls the corresponding template from the spectral population synthesis performed in the visible.

Table 5. Sb galaxy groups

Galaxy	SWP	LWP/R	slit (kpc × kpc)	Spectral Type
Important bulge stellar population and moderate UV flux				
	NGC 224		$\langle 0.03 \times 0.07 \rangle$	
M 31	7	9	0.03×0.07	
Same as NGC 224 with additional weak emission lines				
	G_N4579		$\langle 0.9 \times 1.8 \rangle$	
M 58	2	3	1.2×2.5	T–S 3
M 88	1	—	0.7×1.3	T–S 3
Reddened nuclear starburst				
	G_N7552		$\langle 1.0 \times 2.0 \rangle$	
M 90	—	1	1.0×2.0	T–S 7
NGC 7552	3	1	1.1×2.1	T–S 7
NGC 7582	3	6	1.0×2.0	
Moderate bulge stellar population and moderate UV flux				
	G_N1433		$\langle 0.5 \times 1.0 \rangle$	
NGC 1433	1	1	0.6×1.3	
NGC 2841	1	2	0.4×0.8	
NGC 4102	—	1	0.6×1.1	
Nuclear starburst: flat spectrum				
	G_N1672		$\langle 1.2 \times 2.4 \rangle$	
M 95	1	1	0.5×1.0	T–S 5
NGC 245	1	—	2.6×5.3	
NGC 1097	1	2	0.8×1.6	
NGC 1672	4	1	0.8×1.7	
NGC 2146	—	1	0.6×1.1	
NGC 6300	1	3	0.7×1.4	
NGC 6500	—	1	1.9×3.8	
NGC 6764	2	1	1.5×3.1	
Very blue nuclear starburst				
	G_N7496		$\langle 1.2 \times 2.4 \rangle$	
NGC 3049	2	1	0.9×1.9	
NGC 3504	1	1	1.0×2.0	
NGC 3982	3	1	0.6×1.2	
NGC 5430	6	6	2.0×3.9	
NGC 7496	2	1	1.0×2.0	
NGC 7714	4	1	1.8×3.6	
Important bulge stellar population and moderate UV flux				
	G_N5194		$\langle 0.4 \times 0.8 \rangle$	
M 51	3	1	0.3×0.6	
M 63	—	1	0.3×0.7	
NGC 5005	1	1	0.7×1.3	
Reddened nuclear starburst				
	G_N2903		$\langle 0.2 \times 0.4 \rangle$	
NGC 253	2	2	0.1×0.2	
NGC 2903	3	1	0.4×0.7	T–S 7

Table Notes. Columns 2 and 3 give the number of IUE spectra effectively used; column 4 gives the projected IUE aperture ($10'' \times 20''$) in kpc × kpc.

galaxies: it would produce prohibitively high flux excesses in the region around $\lambda 2200$ Å. At most weak $\lambda 2200$ Å absorptions, like those observed in the LMC, are present in their spectra — see also Kinney et al. (1994) and Paper II.

As an example, we illustrate a synthesis result for the Sc group G_N2997 in Fig. 4. Notice that this group has a significant but not dominant bulge flux contribution. For visualisation purposes, we show in Fig. 4 the individual spectra of the H II region (a) and bulge (d) templates, the sum of the templates LMC I and LMC II (b), and the sum of the templates LMC III, LMC IVA and LMC V (c); these four spectra are shown in their true proportions (in terms of flux fraction at $\lambda 2646$ Å), according to the synthesis.

Below we discuss the synthesis results for each group. We point out that the continuum distributions and the absorption features are in general well reproduced by the synthesis, with the exception, for some cases, of C IV$_{\lambda 1549}$ and Si IV$_{\lambda\lambda 1394,1403}$. These lines are sensitive to metallicity (Leitherer, Robert & Heckman 1995) and are not necessarily of equal strength in the galaxies and the H II region templates.

Hot old stellar population components associated with UV-turnups appear to occur in nuclei of early-type galaxies (Bica et al. 1996 and references therein). In spiral nuclei, this possibility cannot be ruled out, especially when bulge stellar populations dominate like in some Sa galaxies. For the sake of simplicity, we use however in the present syntheses a bulge population with a weak far-UV flux, and flux excesses in this region are accounted for by young-age components. This description is indeed realistic for spiral galaxies.

4.1. Sa galaxy groups

Spectral properties of Sa galaxy groups (Tables 7 and 8) can be accounted for by different contributions of bulge and young populations: the ratio RH II/Bulge contributions (flux at $\lambda 2646$ Å)

Table 6. Sc galaxy groups

Galaxy	SWP	LWP/R	slit (kpc × kpc)	Spectral Type
Moderate bulge stellar population and moderate UV flux				
	G_N2997		$\langle 1.0 \times 2.0 \rangle$	
M 101	4	2	0.1×0.3	
M 106			0.3×0.6	
Mrk 12	2	1	2.6×5.2	
NGC 1667	2	1	2.9×5.9	
NGC 2403	2	1	0.2×0.4	
NGC 2997	3	1	0.7×1.4	T–S 5
NGC 6221	1	1	0.9×1.7	
NGC 7590	1	1	0.9×0.9	
Nuclear starburst: flat spectrum				
	G_N4321		$\langle 1.4 \times 2.8 \rangle$	
M 100	3	3	0.8×1.6	T–S 5
NGC 931	3	1	3.2×6.4	
NGC 3994	1	1	2.0×4.0	
NGC 4244	2	2	0.2×0.3	
NGC 6217	1	—	0.9×1.8	
Blue stellar population				
	G_N598		$\langle 0.1 \times 0.2 \rangle$	
M 33	2	4	0.04×0.08	
NGC 7793	4	4	0.1×0.3	
Very blue nuclear starburst				
	G_N5236		$\langle 1.0 \times 2.0 \rangle$	
M 83	4	7	0.3×0.6	T–S 7
NGC 3310	3	1	0.7×1.3	
NGC 3395	1	—	1.0×2.1	
NGC 7673	1	1	2.2×4.4	

Table Notes. Columns 2 and 3 give the number of IUE spectra effectively used; column 4 gives the projected IUE aperture ($10'' \times 20''$) in kpc × kpc.

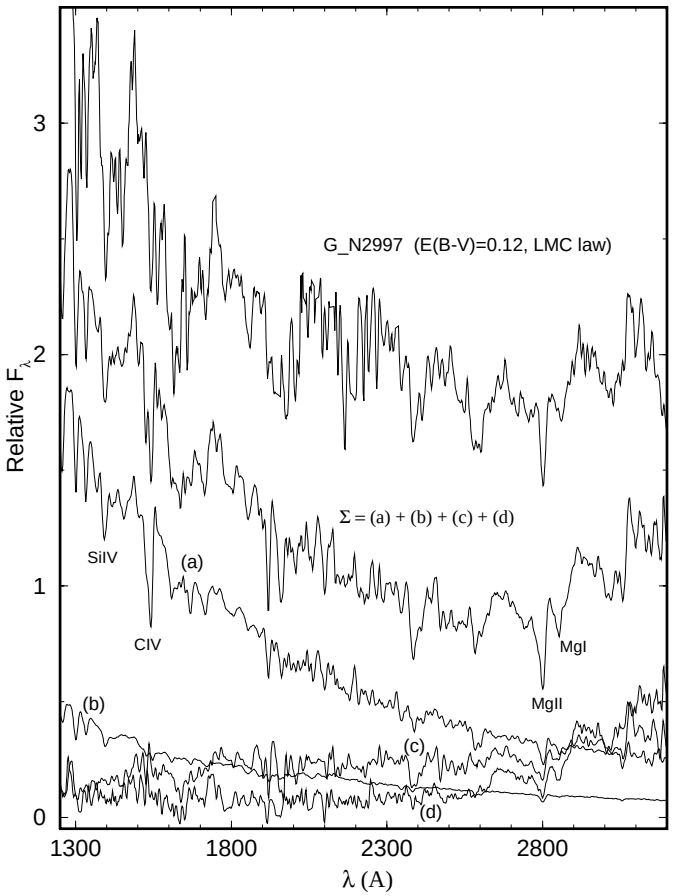

Fig. 4. Stellar population synthesis for the Sc group G_N2997. (a) - H II region template; (b) - sum of the templates LMC I and LMC II; (c) - same as (b) for LMC III, LMC IVA and LMC V; and (d) - bulge. The spectrum at the top is the observed one, de-reddened as indicated. Main absorption features are identified. Units as in Fig. 1.

ranges from 0.09 (NGC 4594) to 5.22 (G_N7130), as can be seen in the syntheses results in Table 9. It is worth pointing out that the spectrum of group G_N1808, albeit among the reddest in Sa galaxies (Fig. 1), is not bulge-dominated like that of NGC 4594. Rather, it has a very important contribution from young components reddened by the largest $E(B-V)$ value in the sample (Table 9).

We show in Fig. 5 the de-reddened spectra of the two extreme cases of UV stellar population detected in Sa galaxies, G_N7130 with the bluest UV spectrum and NGC 4594 with the largest bulge flux contribution, along with the respective synthesized population spectra. Notice that the spectrum of G_N7130 has been reddening-corrected with an SMC law in order to avoid creating a unrealistic $\lambda 2200$ Å bump. As can be seen in Table 1, for the groups with the largest young component flux contributions (G_N7130 and G_N1808), more than 50% of the members are barred galaxies.

4.2. Sb galaxy groups

Sb galaxies present the widest variety of spectral properties. In fact, we have found 8 distinct groups according to relative bulge and young population contributions. The two extreme cases of stellar populations (NGC 224 and G_N7496), together with their respective syntheses, are illustrated in Fig. 6. The population syntheses (Table 9) show that for the G_N7496, G_N1672, G_N7552 and G_N2903 groups the bulge contribution is almost negligible. Their de-reddened spectra increase strongly towards the UV, such as that of G_N7496 (Fig. 6). This slope decreases from G_N7496 to G_N2903 reflecting the relative importance of young bursts contribution to the intermediate age populations. Again let us notice that more than 80% of the galaxies in these groups have bars (Table 2). The remaining Sb groups are characterised by a strong bulge component increasing from G_N5194 to NGC 224. Most galaxies in these groups do not have bars (Table 2). The rôle of bars in triggering star-formation is discussed in Sect. 5.

4.3. Sc galaxy groups

Four different groups have been distinguished for the stellar populations in Sc galaxies (Fig. 3). They are characterised by weak bulge flux contributions (Table 9). As can be seen in Table 9 for Sc groups, flux-fractions are evenly distributed among

Table 7. Equivalent width and continuum measurements for the galaxy groups

		Group —	4594	1808	7130	4736	224	4579	7552	1433	1672	7496	5194	2903	2997	4321	598	5236
UV#	Window (Å)	Main absorbers	Equivalent Widths (Å)															
4	1290–1318	Si II, Si III	4.9	6.4	4.1	8.5	9.5	16.3	11.0	8.5	6.5	5.3	9.0	11.3	10.1	8.8	7.3	4.9
7	1384–1414	Si IV, Fe V	4.6	20.6	10.9	15.6	5.6	17.3	8.8	11.9	9.4	7.4	10.6	10.3	10.0	13.0	8.3	7.8
13	1534–1570	C IV	4.4	21.3	9.6	10.2	1.8	—	13.1	6.7	14.7	7.0	12.0	9.5	7.5	10.2	9.6	9.0
19	1700–1736	N IV, Si IV, Fe IV	8.3	7.6	6.6	8.1	9.0	10.2	5.5	2.1	5.8	3.7	8.3	7.8	3.8	2.5	4.0	4.3
43	2506–2574	Fe I, Si I, Si III	32.8	23.1	9.6	22.2	34.2	20.0	14.3	21.2	9.9	8.3	23.5	10.0	10.3	8.7	13.2	7.8
44	2574–2596	Mn II, Fe II	7.6	11.4	3.9	8.9	12.9	7.7	7.6	11.7	6.1	3.7	8.8	6.5	7.1	3.0	5.9	6.4
45	2596–2642	Fe II, Mn II, Si III	15.3	14.3	4.3	1.0	19.8	12.5	9.0	17.2	5.3	3.6	14.7	3.9	10.1	3.0	7.6	1.8
51	2768–2830	Mg II, Mn II, O V	30.3	20.3	17.1	26.4	34.6	9.1	15.1	27.8	16.6	11.7	23.9	15.3	18.4	12.3	12.1	13.2
52	2830–2900	Mg I, C II, Si I	24.6	13.4	10.8	18.7	30.7	18.7	8.1	21.1	10.2	5.7	24.1	9.9	14.1	6.0	11.3	7.3
λ (Å)			Continuum points — C_λ/C_{2646}															
1282			1.31	0.42	1.38	0.48	1.52	1.45	0.83	2.70	1.11	2.39	1.18	0.81	1.42	1.56	2.51	2.22
1348			1.03	0.35	1.26	0.39	1.09	1.22	0.73	2.15	1.03	2.04	0.89	0.74	1.22	1.49	2.20	2.08
1490			1.04	0.55	1.33	0.60	0.98	1.18	0.82	2.12	1.10	2.06	1.19	0.86	1.32	1.17	2.24	1.93
1768			0.88	0.65	1.20	0.55	0.80	0.97	0.92	1.65	1.04	1.63	1.00	0.91	1.05	1.24	1.77	1.61
2079			0.78	0.61	1.10	0.69	0.55	0.68	0.98	1.50	1.07	1.35	0.81	0.98	1.03	1.16	1.43	1.28
2258			0.63	0.50	0.97	0.62	0.64	0.75	0.89	1.59	1.00	1.12	0.96	0.88	0.91	1.07	1.16	1.16
2466			0.82	0.78	0.92	0.68	0.61	0.77	0.96	1.18	1.00	1.08	1.03	0.89	0.96	1.03	1.06	1.08
2959			2.08	1.38	1.12	1.62	1.85	1.70	1.11	1.89	0.98	0.99	1.68	1.05	1.26	1.00	1.02	0.88
3122			2.47	1.62	1.29	1.88	2.35	2.05	1.25	2.44	1.01	0.99	2.13	1.08	1.35	1.01	1.09	0.85

Table Notes. C IV$_{\lambda 1549}$ and Mg II$_{\lambda\lambda 2796,2803}$ in G_N4579 are contaminated with emission. Uncertainties in EWs are typically $\leq 10\%$, except for bulge-dominated groups shortward of $\lambda < 2000$ Å, where it may amount to $\approx 20\%$ because of weak far-UV flux.

Table 8. Equivalent width and continuum measurements for the base

		Element:	RH II	LMC I	LMC II	LMC III	LMC IVA	LMC V	E2E5
		Age:	2.5 Myr	10 Myr	25 Myr	75 Myr	0.2 Gyr	1.2 Gyr	bulge
UV#	Window	Main absorbers	Equivalent Widths (Å)						
4	1290–1318	Si II, Si III	2.2	4.0	4.2	6.2	5.2	17.9	18.7
7	1384–1414	Si IV, Fe V	5.1	5.2	4.1	3.4	4.5	12.6	14.4
13	1534–1570	C IV	5.4	3.9	2.3	3.4	3.3	10.4	9.7
19	1700–1736	N IV, Si IV, Fe IV	3.9	2.2	2.6	4.0	6.4	11.0	0.2
43	2506–2574	Fe I, Si I, Si III	3.3	3.8	4.2	4.9	7.2	20.3	32.7
44	2574–2596	Mn II, Fe II	5.3	3.4	3.9	2.7	5.2	12.0	12.6
45	2596–2642	Fe II, Mn II, Si III	4.3	3.4	3.4	4.1	4.9	8.6	18.1
51	2768–2830	Mg II, Mn II, O V	8.3	8.6	9.7	11.0	12.2	25.9	34.7
52	2830–2900	Mg I, C II, Si I	5.2	4.0	4.6	5.9	7.1	13.9	26.2
λ (Å)			Continuum points — C_λ/C_{2646}						
1282			5.36	4.50	3.70	2.43	0.79	0.69	1.03
1348			4.63	3.92	3.36	2.35	1.03	0.43	0.71
1490			4.00	3.19	2.87	2.38	1.27	0.78	0.78
1768			2.81	2.11	2.10	1.77	1.28	0.91	0.52
2079			1.84	1.74	1.64	1.62	1.15	1.13	0.49
2258			1.50	1.37	1.27	1.26	1.11	1.03	0.57
2466			1.22	1.18	1.10	1.01	0.94	0.93	0.62
2959			0.83	0.80	0.86	0.89	1.03	1.09	1.92
3122			0.80	0.72	0.83	0.88	1.10	1.27	2.56

Table Notes. RH II is the average of M 101, M 33, LMC and SMC H II regions.

the age components which imply different star-formation histories compared to Sb galaxies, and/or reflect the small size of Sc bulges with respect to the surrounding disc contributions included in the IUE entrance slit. The latter fact cannot be ignored when interpreting the observed spectra of the central regions of the current Sc groups, contrary to Sa and Sb galaxies.

In Fig. 7 we show the de-reddened spectrum of the very blue group G_N5236, along with its synthesised spectrum.

4.4. Metallicity-sensitive absorption features?

As mentioned above, most of the absorption features are well reproduced by the synthesis algorithm. In Table 10 we list the

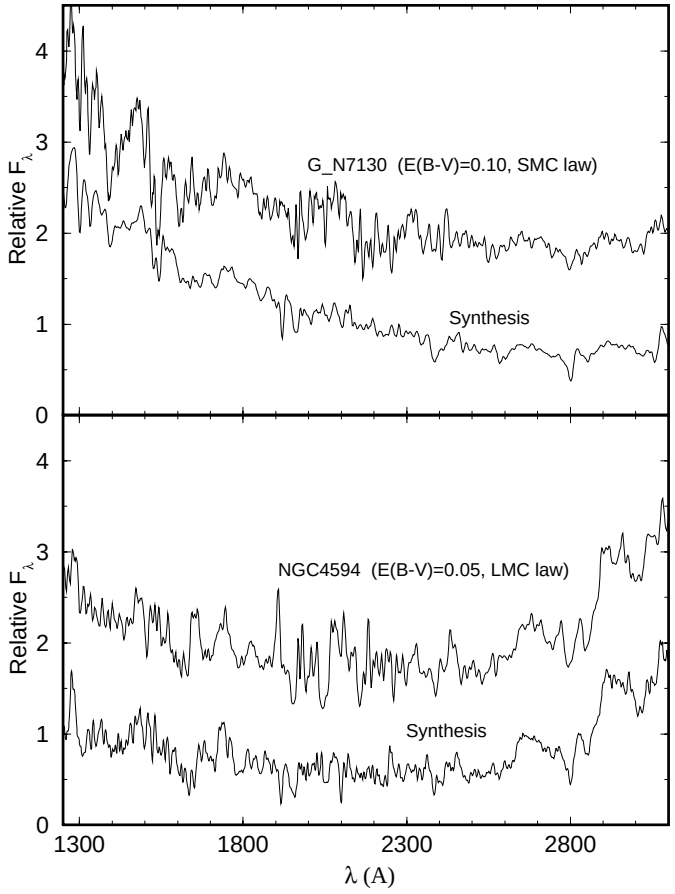

Fig. 5. Stellar population synthesis for Sa groups. Top panel: G_N7130 de-reddened for Galactic extinction with $E(B-V)=0.10$ using an SMC law, compared to its synthesized spectrum; bottom panel: same as above for NGC 4594 corrected with $E(B-V)=0.05$ using an LMC law. Units as in Fig. 1.

Table 9. Stellar population synthesis results

	$\lambda 2646$ Å Flux fraction (%)							
	RH II	LMC	LMC	LMC	LMC	LMC	E2E5	
Group		I	II	III	IVA	V		$E(B-V)$
Sa Groups								
G_N7130	35.2	20.4	1.3	3.4	9.6	23.3	6.7	0.10†
G_N1808	12.3	4.2	2.9	7.6	19.8	41.6	11.5	0.26†
G_N4736	6.1	7.4	6.5	6.5	13.8	30.4	29.2	0.24
NGC 4594	6.6	2.6	6.0	4.8	2.5	6.4	71.2	0.04
Sb Groups								
NGC 224	4.6	3.0	3.9	3.0	2.0	5.7	77.7	0.00
G_N4579	5.2	9.1	6.7	6.9	7.8	4.8	59.3	0.04
G_N1433	10.3	9.1	2.7	3.5	3.4	4.0	67.0	0.00
G_N5194	8.8	7.0	3.6	7.4	11.6	29.8	31.9	0.12
G_N7496	10.4	45.7	4.9	13.2	5.7	19.9	0.2	0.06
G_N1672	7.8	12.9	6.9	12.0	16.0	42.4	1.9	0.10
G_N7552	5.3	17.9	3.9	10.4	27.3	35.1	0.0	0.18
G_N2903	5.9	9.6	7.9	17.3	29.1	29.5	0.8	0.16
Sc Groups								
G_N4321	28.4	32.8	2.1	1.6	3.4	30.4	1.2	0.14
G_N2997	36.4	9.8	1.4	1.5	7.7	22.1	21.0	0.12
G_N598	38.4	14.9	3.0	3.5	13.9	17.4	9.0	0.04
G_N5236	49.7	10.8	2.8	3.4	6.1	25.7	1.4	0.08

Table Notes. † - reddening-corrected using an SMC law.

difference between the EWs measured in the group spectra and those obtained by the synthesis algorithm, for the absorption features used in the syntheses. In general, the synthesized EWs of Si IV$_{\lambda\lambda 1394,1403}$ and C IV$_{\lambda 1549}$ are smaller than the observed ones by 30 to 50%; in such cases, these features were not included as constraints in the synthesis. As can be seen in Table 10, groups in which young components dominate (i.e. bulge fractions $\leq 15\%$ at $\lambda 2646$ Å) have important positive residuals at Si IV$_{\lambda\lambda 1394,1403}$ and C IV$_{\lambda 1549}$. Leitherer, Robert & Heckman (1995) showed that these lines are very sensitive indicators of the presence of massive O and B stars. A possible explanation for the fact that our synthesis does not reproduce well the EW of these features in most central regions of spiral galaxies containing recent star-formation is that these starbursts are more metal-rich (above solar) than the base elements used in the synthesis; we recall that the base elements between 10 and 500 Myr are from LMC clusters, and the H II region template is an average of SMC, LMC, M 33 and M 101 H II regions, all with a fairly low metallicity.

We present in Fig. 8 relations involving EW(Si IV), EW(C IV), EW(Mg II) and internal $E(B-V)$, where we distinguish the galaxy morphological types. Groups with important bulge flux contribution ($\geq 15\%$ at $\lambda 2646$ Å) are shown as filled symbols, and those with important recent star-formation, as open symbols. The top panel confirms the common origin of the C IV$_{\lambda 1549}$ and Si IV$_{\lambda\lambda 1394,1403}$ absorption features. The middle panel shows a good correlation between EW(C IV) and reddening, especially for galaxy groups dominated by recent star-formation. As shown in the bottom panel, a similar dependence is also apparent for EW(Mg II); however, this correlation fails for bulge-dominated groups for which Mg II$_{\lambda\lambda 2796,2803}$ arises mainly from the old stellar population. For groups dominated by recent star-formation (Fig. 8), Sc galaxy groups tend to have smaller EWs, while Sa's tend to have larger ones. All the evidence above is consistent with the scenario of higher metallicity gas generating star bursts as one goes from Sc's to Sa's. The correlation of EWs with reddening also suggests increasing dust contents from Sc's to Sa's, which would be expected from higher metallicity. A simpler, alternative explanation for this correlation is that to produce a massive starburst, large amounts of interstellar matter have to be gathered in the center of a galaxy, hence increasing the extinction.

4.5. UV extrapolation of optical population syntheses

A stellar population synthesis of some of these galaxies has been made from optical spectroscopy by Bica (1988). We show in Fig. 9 the visible/near-infrared synthesis of the group S 7 of Bica (1988), and its extrapolation to the UV. In order to check the consistency of the syntheses in the optical and UV ranges, we compare in Fig. 10 the UV extrapolation of the visible/near-infrared synthesis of the S 7 group (Bica 1988) with the present

Table 10. Equivalent width residuals

Group	Bulge Fraction (in %)	EW(measured) – EW(synthesis) (in Å) UV#4 Si II	UV#7 Si IV	UV#13 C IV	UV#19 N IV	UV#43 Fe I	UV#44 Mn II	UV#45 Fe II	UV#51 Mg II	UV#52 Mg I
Sa groups										
G_N7130	6.7	0.0	5.3	4.4	2.3	0.6	−2.8	−1.7	1.3	1.0
G_N1808	11.5	−0.6	14.1	15.6	1.6	9.1	2.9	6.6	−0.5	0.5
G_N4736	29.2	0.2	8.6	−0.1	3.1	5.5	0.0	−8.6	2.4	2.3
NGC 4594	71.2	−5.9	−4.3	−2.0	5.6	8.6	−2.9	1.0	0.0	1.9
Sb groups										
NGC 224	77.7	−2.6	−4.2	−5.2	6.7	8.0	1.9	4.6	3.1	7.1
G_N4579	59.3	7.3	9.6	−5.5	7.3	−0.5	−1.6	−0.1	−18.7	−2.0
G_N1433	67.0	−0.6	3.7	0.5	−0.5	−1.1	1.8	3.6	−1.4	−0.9
G_N5194	31.9	0.8	3.4	6.1	3.4	6.3	−0.3	4.7	−0.7	7.2
G_N7496	0.2	0.8	2.2	2.6	0.0	1.2	−1.5	−1.1	−1.3	−1.2
G_N1672	1.9	0.4	3.6	9.6	0.3	−1.7	−1.4	−0.9	−1.3	0.2
G_N7552	0.0	5.2	3.2	8.3	0.1	4.0	0.7	3.3	−1.2	−0.8
G_N2903	0.8	5.4	5.1	5.0	2.5	0.2	0.0	−1.7	−0.5	1.1
Sc groups										
G_N4321	1.2	4.7	7.4	5.1	−1.7	0.1	−3.5	−2.4	−2.5	−2.2
G_N2997	21.0	5.4	3.9	1.9	−0.5	−2.0	−0.7	2.1	−1.7	0.3
G_N598	9.0	3.4	2.8	4.4	−0.3	4.4	−0.6	1.4	−3.6	1.2
G_N5236	1.4	1.4	2.4	3.6	−0.2	−0.1	−0.2	−3.6	−0.9	−0.9

Table Notes. Column 2: percentage bulge fraction with respect to flux at $\lambda 2646$ Å.

UV synthesis of the group G_N5236, which is the UV counterpart of group S 7. We emphasise that both groups include as a principal member the nuclear starburst galaxy NGC 5236 (M 83). In spite of aperture differences, there is a good agreement.

Since the optical and IUE slits sample different spatial regions, the agreement between the extrapolated optical synthesis spectrum and the observed UV synthesis one will depend on the ratio of bulge to disc population contributions inside the large IUE entrance. Indeed, in the case considered the contribution from the intermediate age I 1/I 2 component (1–5 Gyr) is larger in the IUE spectral synthesis, as expected from a more important disc component.

In summary we conclude that the IUE spectral range contains enough information on spectral distribution and absorption features to allow a population synthesis to be performed in a constrained way. However, the ideal method will be to perform overall syntheses through equal aperture in the range $1\,000 - 10\,000$ Å, using e.g., HST data.

4.6. Star-formation history

The synthesis results (Table 9) refer to flux fractions; in order to discuss star-formation histories, it is useful to convert these values into mass fractions. Previous synthesis results in the visible/near-infrared ranges (Bica 1988) have been converted into mass fractions by means of mass-to-light ratios M/L_V computed from a stellar evolution model of star clusters (Bica, Arimoto & Alloin 1988). Complete details on this modeling, such as the IMF slope and the lower and upper cutoffs, are provided in that paper. We recall in Table 11, for each age component used in the present paper, the corresponding age interval and mass-to-light ratio expressed in luminosity at $\lambda 5870$ Å. Using our 1 000–10 000 Å stellar population templates we measured the ratio L_{5870}/L_{2646}, and derived the mass-to-light ratio M/L_{2646}, respectively shown in columns 4 and 5 of Table 11.

Table 11. Mass-to-light ratios

Component	Age interval (10^9 yr)	$\frac{M}{L_{5870}}$	$\frac{L_{5870}}{L_{2646}}$	$\frac{M}{L_{2646}}$
R HII	0.0–0.007	0.035	0.14	0.005
LMC I	0.007–0.02	0.007	0.28	0.002
LMC II	0.02–0.07	0.063	0.41	0.026
LMC III	0.07–0.2	0.305	0.65	0.198
LMC IVA	0.2–0.7	0.343	1.60	0.548
LMC V	0.7–7.0	2.270	3.00	6.820
E 2E 5	7.0–17.0	8.260	19.10	157.7

Then, mass fractions can be derived from the synthesis flux fractions by means of M/L_{2646}. The results are shown in Table 12.

In terms of mass fractions, the bulge dominance in Sa galaxies is clear, even for the groups in which the UV light is dominated by recent star-formation or old but blue stars. The Sb galaxies with UV light dominated by recent star-formation (groups G_N7496, G_N1672, G_N7552 and G_N2903), still have a negligible mass fraction stored in the young components, so that the old disk and bulge appear to have comparable and dominant mass contributions. The latter conclusion is valid as well for the Sc galaxies, in spite of their smaller bulge sizes.

Rough estimates of total (dynamical) masses can be obtained using rotation curves of typical Sa, Sb and Sc galaxies in

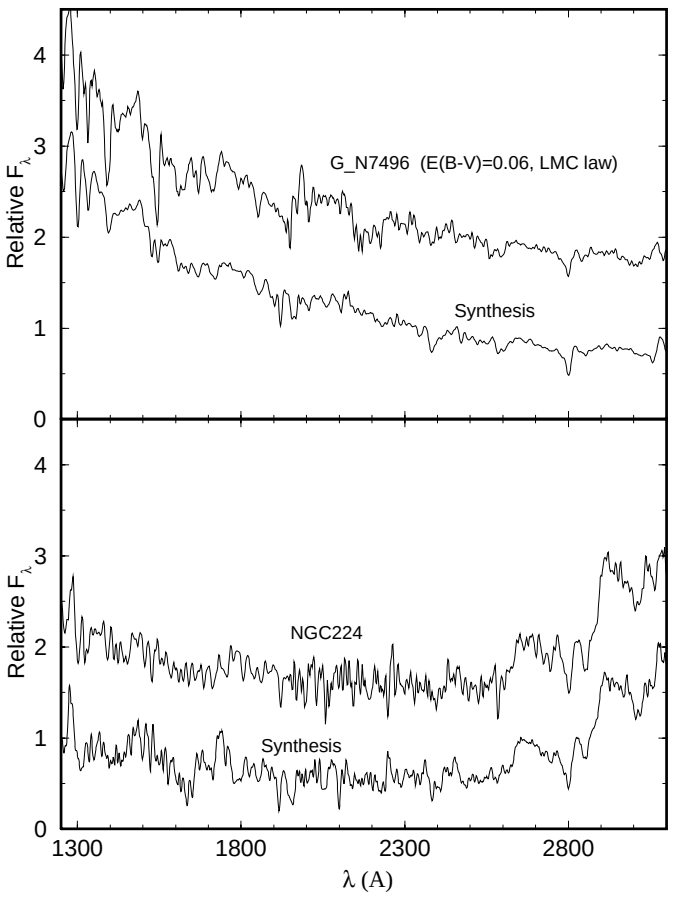

Fig. 6. Stellar population synthesis for Sb groups. Top panel: G_N7496 de-reddened with $E(B-V)=0.06$ using an LMC law compared to its synthesised spectrum; bottom panel: same as above for NGC 224 with no reddening correction. Units as in Fig. 1.

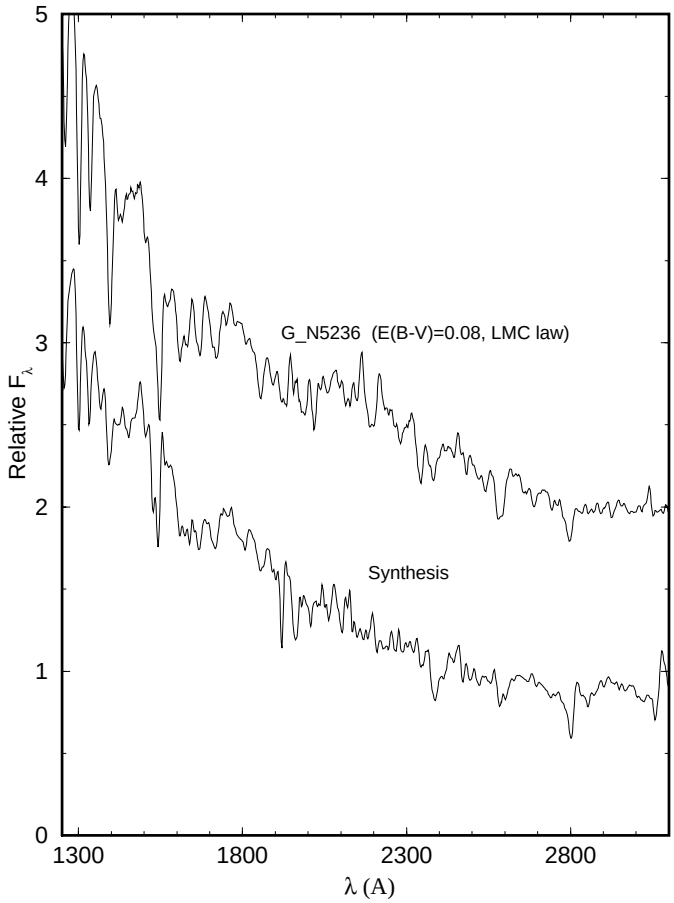

Fig. 7. Stellar population synthesis for the Sc group G_N5236 de-reddened with $E(B-V)=0.08$ using an LMC law compared to its synthesised spectrum. Units as in Fig. 1.

Rubin et al. (1985, their Fig. 6). Typically, the central kpc (in radius) contains 2.3×10^9, 1.9×10^9 and $0.9\times10^9\,M_\odot$, respectively for Sa, Sb and Sc galaxies. Considering the young stellar components (RH II to LMC IVA, $t\leq500$ Myr), the masses involved in the bursts observed in the blue groups are 1.3×10^7, 8.4×10^7 and $5.5\times10^6\,M_\odot$, respectively for Sa, Sb and Sc galaxies.

Dividing mass fractions (Table 12) by the age intervals (Table 11) corresponding to the components, and using the dynamical masses estimated for Sa, Sb and Sc galaxies, one can calculate the star-formation rate as a function of age. The results are shown in Fig. 11. For each panel we further averaged galaxy groups according to similar star-formation histories. The Sa groups present by far the highest early star-formation rate corresponding to their strong bulges; even for the group G_N7130, with strong star-formation (in terms of UV flux), the overall history does not differ much from those of the bulge-dominated Sa groups. For the bulge-dominated Sb groups, the same conclusion applies. On the other hand, for the Sb groups with strong recent star-formation (in terms of UV flux), also the intermediate age component, probably associated to the disc of these galaxies, appears to have enhanced star-formation rates; this might be related to the high frequency of bars in those groups as discussed in Sect. 5. The Sc groups, as seen through the IUE aperture, are all dominated by high recent star-formation rates, comparable to that of the bulge itself, which might be related to the intrinsic small bulge size, entirely contained in the aperture.

5. On the relation between bars and nuclear bursts

For the subset of Sb galaxies, our sample is large enough (28 objects) to investigate the potential influence of a bar in a galaxy on boosting star-formation. We have divided the 8 Sb groups according to the proportion of barred galaxies in each group. In the upper part of Fig. 2, we display the 4 groups for which the proportion of barred galaxies is less than 70%, while in its lower part, we display the UV spectra of the 4 groups in which the proportion of barred galaxies amounts to 80%–100%. These 4 latter groups are also flux-dominated by CNBs (formerly classified as hot spot nuclei): their observed spectrum over the 1200–3000 Å range is rather flat (except G_N7496 which is even bluer). On the contrary, the 1200–3000 Å spectra of groups in the upper part of Fig. 2 are rising to the red, showing a dominance of the old stellar population (Table 9). After reddening correction, as derived from the syntheses (Table 9), the spectra of the groups

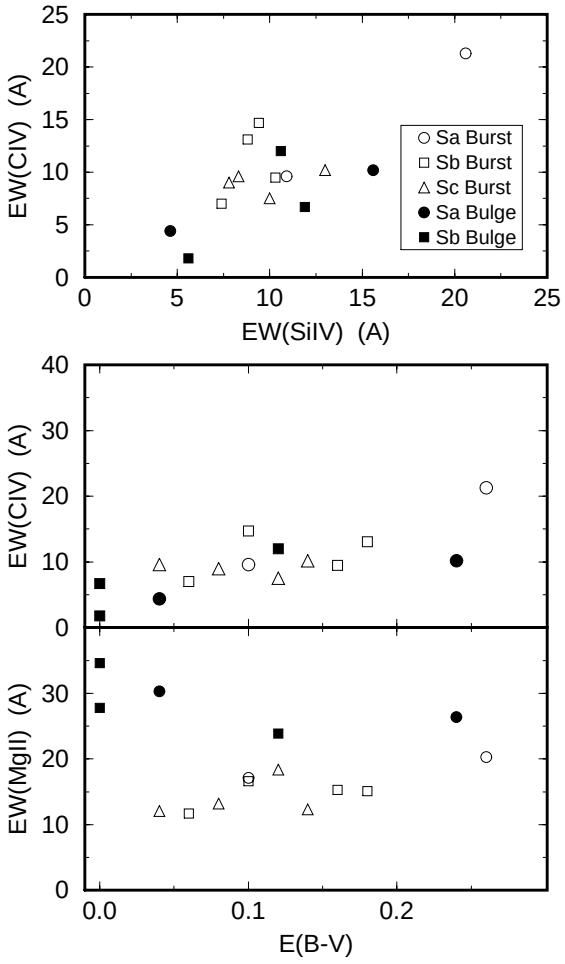

Fig. 8. Relations involving EWs and internal $E(B-V)$. The filled symbols indicate groups with important bulge contribution, and the open ones indicate the groups with important recent star-formation.

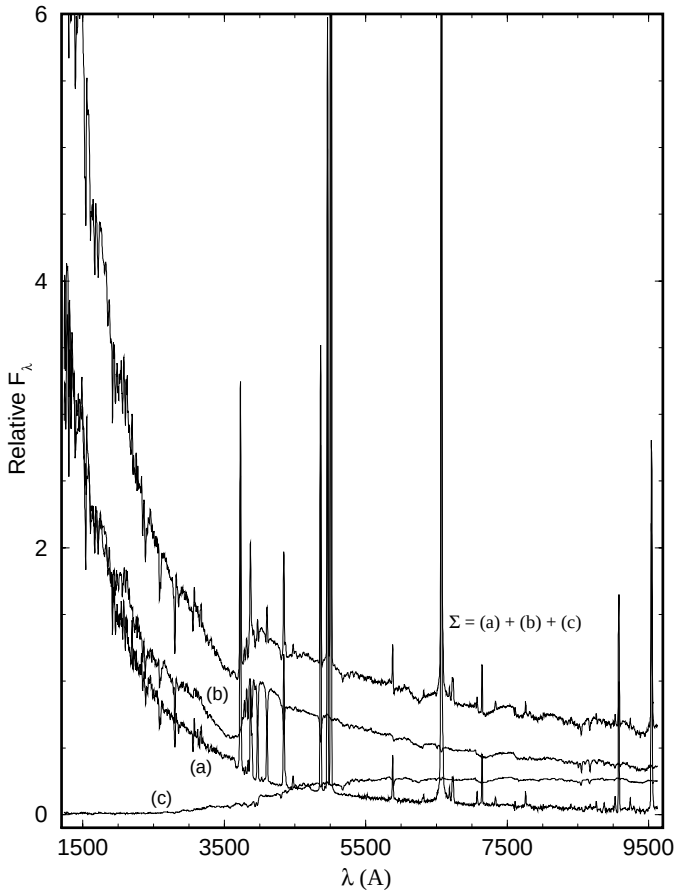

Fig. 9. Visible/near-infrared synthesis of the S 7 group and its extrapolation to the UV. (a) - H II region template (12% at $\lambda 5870$ Å); (b) - sum of the templates LMC I, LMC II, LMC III, LMC IVA (62%); and (c) - same as (b) for LMC V and the bulge (26%). Spectra (a), (b) and (c) are shown in the true proportion (flux fraction) according to the synthesis. Notice that the bulge population flux is nearly negligible for $\lambda < 3000$ Å. Units as in Fig. 1.

with a dominance of barred galaxies turned out to be considerably bluer, like that of G_N7496.

The observed association of bars with CNBs in our sample of Sb galaxies emphasises once more the rôle that a bar can play in driving material towards the center and subsequently forming CNBs.

In the case of grand-design barred spirals, the occurrence of two inner Lindblad resonances (ILR), is a factor favouring the formation of CNBs. In fact, matter expelled in the course of stellar evolution from stars forming the bars will be driven to the region located between both ILRs, where it will build up a ring. As soon as the gas density in this ring exceeds the local virial density in the region, star-formation will proceed and lead to the CNBs. The time it will take for gas in the ring to be exhausted by CNB formation is expected to be quite small. On the other hand, the time for replenishment of gas in the ring, from stellar evolution of stars in the bar, is of the order of 1 Gyr (e.g. Elmegreen 1996). Therefore, we may expect CNB activity to take place with a recurrence of ≈1 Gyr. The predicted picture is then that the CNB should bear the signature of "instantaneous" star-formation and form a sequence of discrete aged components with delays of a few Gyr. This scenario is consistent with the results of our syntheses (Table 9), which suggest that for the groups dominated by barred galaxies, about 65% of the stellar population (in terms of flux contribution) has been formed in the last 500 Myr, while the remaining $\approx$ 35% are of intermediate age from 1 to 5 Gyr (see also Fig. 11 for corresponding star-formation rates). The bulge contribution (flux at $\lambda 2646$ Å) to these groups is almost negligible because the light we observe through the IUE aperture is strongly dominated by CNBs and intermediate age populations (disc). In terms of mass, the young components store about $\approx 10^7\,M_\odot$, which should provide constraints for bar-driving models. The mass involved in the whole CNB is also consistent with the presence of some super-star clusters with masses $10^5 - 10^6\,M_\odot$, considered to be young globular clusters (e.g. Meurer et al. 1995).

6. Conclusions

We have studied the stellar populations in the central parts of nearby spiral galaxies using UV spectra obtained with IUE. The

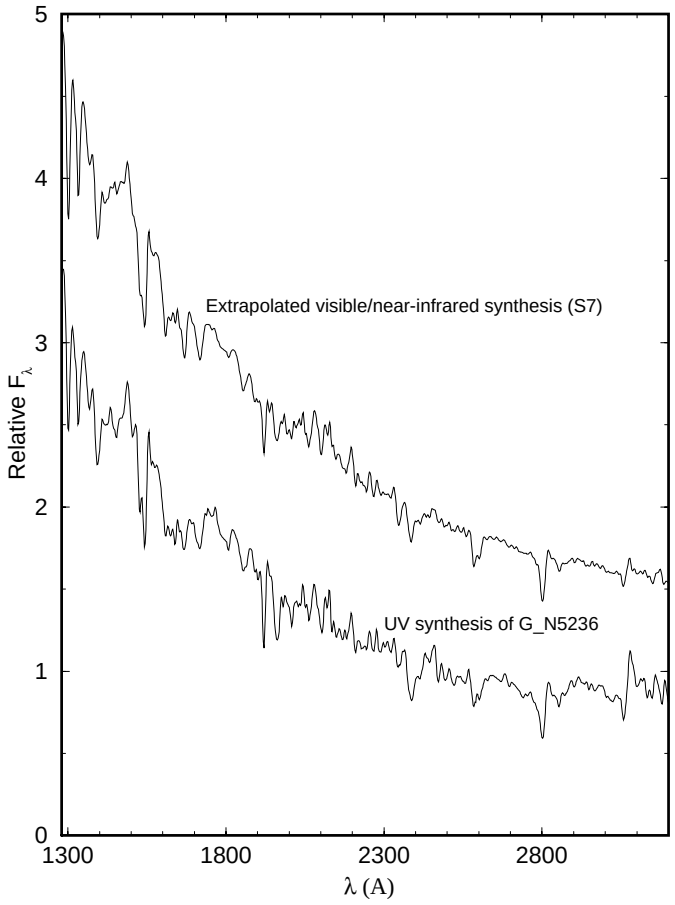

Fig. 10. Comparison in the UV range of the visible/near-infrared synthesis of the S 7 group (Bica 1988) with the present UV synthesis of the group G_N5236. Spectra are normalised at $\lambda 2646$ Å, and the upper one has been shifted arbitrarily. Units as in Fig. 1.

spectra have been grouped according to similarities in morphological types and in spectral feature characteristics. We end up with 4 high (S/N) ratio groups for Sa galaxies, 8 for Sb and 4 for Sc ones. A stellar population synthesis algorithm accounts for this variety of spectral types as due to different mixtures of bulge, circumnuclear burst and disc populations within the area sampled by the IUE aperture ($10'' \times 20''$). From the synthesis it is also possible to derive the internal reddening and to infer the associated extinction law. However, a complicating factor to derive the reddening law in external galaxies is that for most objects, the IUE aperture gathers light from differently reddened spatial regions, which makes the extinction look greyer and tends to wipe out extinction-associated features.

It is interesting to point out that, according to our synthesis, in no case the Galactic reddening law is suitable to describe external galaxies. Our observations, and in particular the weakness of the $\lambda 2200$ Å absorption feature, rather call for the use of the LMC and SMC reddening laws, confirming results obtained for other galaxies (Kinney et al. 1994, Bonatto et al. 1996, Schmitt et al. 1997). It is also worth mentioning that the reddening inferred from the stellar population synthesis in the UV is relatively small, and it is expected that reddening estimates in the infrared for the same galaxies will be much larger. Recently, such an effect was observed in NGC 5128 (Centaurus A; Storchi-Bergmann et al. 1997). Another case is the merger NGC 6240 in which the reddening inferred from the optical stellar population synthesis is $A_V \approx 1.5$ (Schmitt, Bica & Pastoriza 1996), while in the infrared it amounts to $A_V \approx 15$ (Rieke et al. 1985). This is interpreted in the sense that different wavelengths probe different depths (shorter wavelength flux coming from more external regions) and that consequently, different stellar populations might be sampled.

Table 12. Synthesis results in terms of mass fractions

	Mass fraction (%)						
Group	RH II	LMC I	LMC II	LMC III	LMC IVA	LMC V	E2E5
Sa Groups							
G_N7130	0.01	<0.01	<0.01	0.05	0.43	13.01	86.49
G_N1808	<0.01	<0.01	<0.01	0.07	0.51	13.45	85.96
G_N4736	<0.01	<0.01	<0.01	0.03	0.16	4.30	95.51
NGC 4594	<0.01	<0.01	<0.01	0.01	0.01	0.39	99.59
Sb Groups							
NGC 224	<0.01	<0.01	<0.01	<0.01	0.01	0.32	99.67
G_N4579	<0.01	<0.01	<0.01	0.01	0.05	0.35	99.59
G_N1433	<0.01	<0.01	<0.01	0.01	0.02	0.26	99.72
G_N5194	<0.01	<0.01	<0.01	0.03	0.12	3.88	95.97
G_N7496	0.03	0.05	0.08	1.51	1.80	78.33	18.20
G_N1672	0.01	<0.01	0.03	0.40	1.46	48.18	49.92
G_N7552	0.01	0.02	0.04	0.80	5.80	92.73	<0.61
G_N2903	0.01	0.01	0.06	0.99	4.60	57.58	36.36
Sc Groups							
G_N4321	0.04	0.02	0.01	0.08	0.47	51.96	47.43
G_N2997	0.01	<0.01	<0.01	0.01	0.12	4.35	95.52
G_N598	0.01	<0.01	0.01	0.04	0.49	7.67	91.77
G_N5236	0.06	<0.01	0.02	0.17	0.83	43.77	55.14

We presented far-UV flux and mass fractions of the different age components found in the syntheses, inferring also on the star-formation histories and absolute masses involved. In Sa galaxies, and some Sb ones, the bulge stellar population dominates the mass, and even the UV flux. On the other hand, in some Sb and Sc galaxies, the intermediate-age population associated to the disc appears to have far-UV flux contributions larger than that of the bulge. The mass stored in the central parts (1–2 kpc) of spirals with important recent star-formation ($t \leq 500$ Myr) typically amounts to $\approx 10^7\, M_\odot$ only. The star-forming events occur preferentially in barred spirals; this favours a scenario in which material is driven along the bar towards the central regions, where it accumulates and triggers star-formation.

The stellar population templates and the methods emphasized in the present study will be valuable tools for the analysis and interpretation of UV spectra of distant galaxies, which can be obtained with HST.

Acknowledgements. We are grateful to Dr. J. Lequeux for some helpful comments on the text. We thank PROPESQ–UFRGS for partially supporting Dr. D. Alloin during her stay in Porto Alegre. We acknowledge CNPq and FINEP for partially supporting this work.

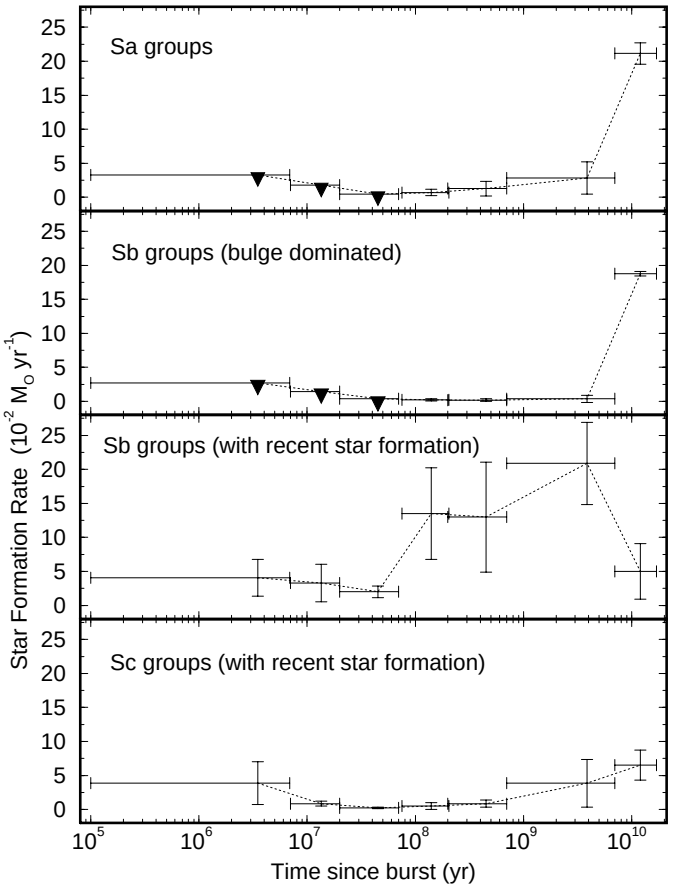

Fig. 11. Average star-formation rates in the central kpc of various spiral groups. Horizontal bars represent event duration. Vertical bars represent the internal dispersion within the groups. Black triangles indicate upper limits.

References

Alloin, D. & Bica, E. 1990, RMxAA, 21, 182

Athanassoula, E. 1992, MNRAS, 259, 328

Barth, A.J., Ho, L.E., Filippenko, A.V. & Sargent, W.L.W. 1995, AJ, 110, 1009

Bica, E. & Alloin, D. 1987a, A&AS, 70, 281

Bica, E. & Alloin, D. 1987b, A&A, 186, 49

Bica, E. 1988, A&A, 195, 76

Bica, E., Arimoto, N. & Alloin, D. 1988, A&A, 202, 8

Bica, E., Alloin, D. & Schmitt, H. 1994, A&A, 283, 805

Bica, E., Bonatto, C., Pastoriza, M.G. & Alloin, D. 1996, A&A, 313, 405

Bonatto, C., Bica, E. & Alloin, D. 1995, A&AS, 112, 71 (Paper I)

Bonatto, C., Bica, E., Pastoriza, M.G. & Alloin, D. 1996, A&AS, 118, 89 (Paper II)

de Vaucouleurs, G., de Vaucouleurs, A., Corwin, H.G. Jr. et al. 1991, *Third Reference Catalogue of Bright Galaxies, Springer-Verlag, New York* (RC3)

Ellis, R.S., Gondhalekar, P.M. & Efstathiou, G. 1982, MNRAS, 201, 223

Elmegreen, B.G. 1996, in *Cold dust and galaxy morphology*, ed. D. Block, Dordrecht: Kluwer, in press

Ferguson. H.C. & Davidsen, A.F. 1993, ApJ, 408, 92

Fitzpatrick, E.L., 1986, AJ, 92, 1068

Kinney, A.L., Bohlin, R.C., Calzetti, D., Panagia, N., Wyse, R.F.G., 1993, ApJS, 86, 5

Kinney, A.L., Calzetti, D., Bica, E. & Storchi-Bergmann, T. 1994, ApJ, 429, 172

Leitherer, C. et al. 1996, PASP, 108, 996

Leitherer, C., Robert, C. & Heckman, T.M. 1995, ApJS, 99, 173

Maoz, D. et al. 1996, AJ, 111, 2248

Martin, P. 1995, AJ, 109, 2428

Mazzarella, J.M. & Balzano, V.A. 1986, ApJS, 62, 751

Meurer, G.R. et al. 1995, AJ, 110, 2665

Pastoriza, M.G. 1975, Ap&SS, 33, 173

Piner, B.G., Stone, J.M. & Teuben, P.J. 1995, ApJ, 449, 508

Prévot, M.L., Lequeux, J., Maurice, E., Prévot, L. & Rocca-Volmerange, B. 1984, A&A, 132, 389

Rieke, G.H., Cutri, R.M., Black, J.H., Kailey, W.F., McAlaray, C.W., Lebofsky, M.J. & Elston, R. 1985, ApJ, 290, 116

Rosa, M., Joubert, M. & Benvenutti, P. 1984, A&AS, 57, 361

Rubin, V.C., Burstein, D., Ford, W.K., Jr. & Thonnard, N. 1985, ApJ, 289, 81

Sandage, A. & Tammann, G.A. 1981 *The Revised Shapley-Ames Catalog*, Carnegie Inst. Washington, Publ. No. 635

Schmitt, H.R., Kinney, A.L., Calzetti, D. & Storchi-Bergmann, T. 1997, AJ, 114, 592

Schmitt, H.R., Bica, E. & Pastoriza, M.G. 1996, MNRAS, 278, 965

Seaton, M.J., 1979, MNRAS, 187, 73p

Storchi-Bergmann, T., Bica, E., Kinney, A.L. & Bonatto, C. 1997, MNRAS, 290, 231

Welch, G.A. 1982, ApJ, 259, 77